Recovering Structure Uncertainties from Noisy Sense Data

Tarek M. Sobh and Ausif Mahmood

Department of Computer Science and Engineering
University of Bridgeport
169 University Avenue
Bridgeport, CT 06601

Abstract

This work examines closely the possibilities for errors, mistakes and uncertainties in sensing systems. We identify and suggest techniques for modeling, analyzing, and recovering these uncertainties. This work concentrates on uncertainties in visual sensing for manipulators. The goal is to recover 3-D structure and motion characteristics of the environments under observation from noisy measurements. We also conjecture that the approaches described here are suitable for other sensors and parameters to be recovered. The computed uncertainties are utilized for reconstructing the geometry, motion parameters, and structure parameters under observation.

1 Introduction

In this work we discuss uncertainty modeling for sensor systems. In particular, we describe some techniques for measuring and computing the uncertainties in recovering some visual parameters. We concentrate on presenting the sources of uncertainty in two dimensional visual data. Then we proceed to identify methods by which the 2-D uncertainty could be transformed into meaningful 3-D interpretations that the observer can use reliably in order to recover the world events. Those methods can be generalized for other sensing problems and parametric recovery from sense data.

Figure 1 depicts the sequence of steps that are to be performed in order to recover the full world uncertainty from 2-D measurements on the image plane. We start by recognizing the sensor uncertainty, then we recover the uncertainty resulting from the image processing technique that is used, the resulting 2-D uncertainties are then refined and used to determine the 3-D models. In the following sections we discuss this sequence.

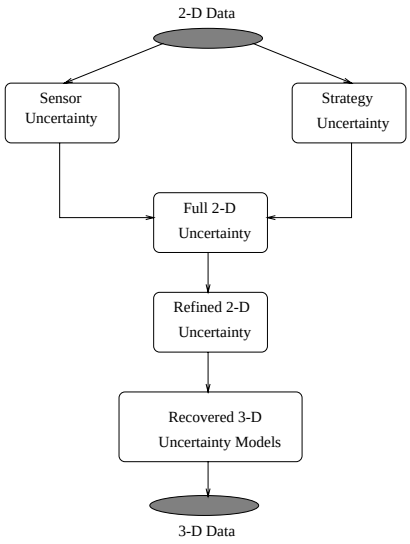

Figure 1: Propagation of Uncertainty

2 Sensor and Image Processing Uncertainties

In this section we develop and discuss modeling the uncertainties in 2-D feature displacement vectors. There are many sources of errors and ways to model uncertainties in image processing and sensing in general [5,8,15,16]. The uncertainty in the recovered values results from sensor uncertainties, noise, and the image processing techniques used to extract and track world features. When dealing with measurements of any sort, it is always the case that the measurements are accompanied by some error. Mistakes also occur, where mistakes are not large errors but failures of a system component or more. A description of errors, mistakes can be found in [2,3].

2.1 Image Formation Errors

There is a need to register errors in mapping from the 3-D world features to the 2-D domain which we use in forming 3-D hypothesis about the scene under observation. The accuracy, precision and modeling uncertainty of the camera (as our sensor, in this case) is an important issue and the first step towards forming a full uncertainty model for recovering the 3-D scene. In figure 2 (redrawn from [3]), a model of the image formation process is illustrated, which lists some salient features of each component. As a lot of the image processing algorithms compute derivatives of the intensity function, noise in the image will be amplified and propagated throughout the observation process. The goal of this treatment is to find a distribution for the uncertainty of mapping a specific 3-D feature into a specific pixel value. In other words, if the feature 2-D position was discovered to be (i, j), then the goal is to find a 2-D distribution for i and j, assuming that there is no uncertainty in the technique used to extract the 2-D feature.
The end product of modeling the sensor uncertainty is to be able to assert the following:

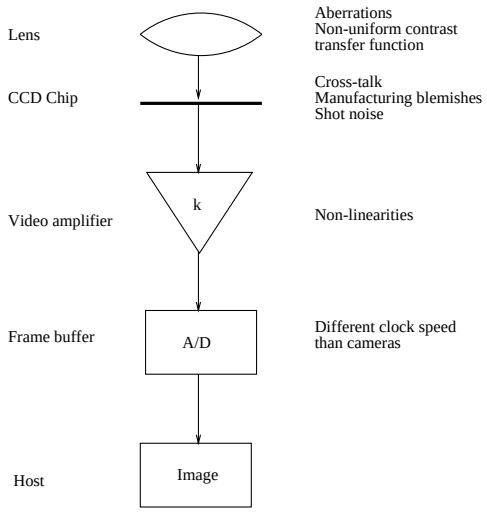

Figure 2: Image Formation

"The 3-D feature F is located in the 2-D pixel position (i, j) with probability p_1 or located in the 2-D pixel position $(i, j+1)$ with probability p_2 or .... *given* that the registered location is (l, m), such that $p_1 + p_2 + ... + p_n = 1$, and $\nexists$ error in the 2-D feature recovery mechanism." The errors in the image formation process are basically of two different kinds. The first type is a spatial error, the other type is a temporal error. The spatial error due to the noise characteristics of a CCD transducer can be due to many reasons, among which are dark signatures and illumination signatures. The technique to be used is to take a large number of images, we can denote the image intensity function as a 3-D function $I(u, v, t)$, with spatial arguments u and v and temporal argument t. The sample mean of the image intensities over N time samples can be denoted by $\overline{I}(u, v)$.

$$\overline{I}(u, v) = \frac{1}{N} \sum_{t=1}^{N} I(u, v, t)$$

The spatial variance in a 5×5 neighborhood of the means is computed by:

$$s^2(u, v) = \sum_{i=-2}^{2} \sum_{j=-2}^{2} (\overline{I}(u + i, v + j) - \overline{I}(u, v))^2$$

The dark signature of the camera can be determined by computing $\overline{I}(u, v)$ of each pixel with the lens cap on. It will be found that a small number of pixels will have non-zero mean and non-zero variance. The specific pixel locations are blemished and should be registered. The uniform illumination is computed by placing a nylon diffuser over the lens and computing the mean and variance. It will be noticed that due to digitizing the CCD array into a pixel array of different size, and the difference in sample rates between the digitizer and camera, the border of the image will have different mean and variance from the interior of the image. Some "stuck" pixels at the location of the blemished pixels will also be noted. The contrast transfer function will also be noted to vary at different distances from the center of the lens.

Temporal noise characteristics can also be identified by taking a number of experiments and notice the time dependency of the pixels intensity function. In our treatment and for our modeling purposes we concentrate on the spatial distribution of noise and its effect on finding the 2-D uncertainty in recovering a 3-D feature location in the pixel array.

2.2 Calibration and Modeling Uncertainties

Methods to compute the translation and rotation of the camera with respect to its coordinates, as well as the camera parameters, such as the focal length, radial distortion coefficients, scale factor and the image origin, have been developed and discussed in the literature [4,10,14]. In this section we use a static camera calibration technique to model the uncertainty in 3-D to 2-D feature locations. In particular we use the sequence of steps used to transform from 3-D world coordinates to computer pixel coordinates in order to recover the pixel uncertainties, due to the sensor noise characteristics described previously.

A sequence of calibration steps is used for a coplanar set of points in order to obtain the rotation and translation matrices, in addition to the camera parameters. The input to the system are two sets of coordinates, (X_f, Y_f), which are the computer 2-D pixel image coordinates in frame memory and (x_w, y_w, z_w), which are the 3-D world coordinates of a set of coplanar points impressed on a piece of paper with known inter-point distances. A discussion of the exact mathematical formulation of the inter-step computations to find all the parameters can be found in [4].

Our approach is to treat the whole camera system as a black box and make input/output measurements and develop a model of its parametric behavior. The next step is to utilize the recovered camera parameters and the number of 3-D points which we created in order to formulate a distribution of the 2-D uncertainty.

The points used in calibration and later in recovering the distribution can be the actual features in the scene that are to be recovered and thus providing a similar experimental environment to the one that the camera will operate in.

The strategy used to find the 2-D uncertainty in the features 2-D representation is to utilize the recovered camera parameters and the 3-D world coordinates (x_w, y_w, z_w) of the known set of points and compute the corresponding pixel coordinates, for points distributed throughout the image plane a number of times, find the actual feature pixel coordinates and construct 2-D histograms for the displacements from the recovered coordinates for the experiments performed. The number of the experiments giving a certain displacement error would be the z axis of this histogram, while the x and y axis are the displacement error. Different histograms can be used for different 2-D pixel positions distributed throughout the image plane. The three dimensional histogram functions are then normalized such that the volume under the histogram is equal to 1 unit volume and the resulting normalized function is used as the distribution of pixel displacement error, thus modeling the sensor uncertainty. The black box approach is thus used to model errors in a statistical sense.

2.3 Image Processing Uncertainties

In this section we describe a technique by which developing uncertainties due to the image processing strategy can be modeled. In addition, we end the discussion by combining both the sensor uncertainties developed in the previous section and the models developed in this section to generate distribution models for the uncertainty in estimating 2-D motion vectors. These models are to be used for determining the full uncertainty in recovering the 3-D scene under observation.

We start by identifying some basic measures and ideas that are used frequently to recognize the behavior of basic image processing algorithms and then proceed to describe the technique we use in order to compute the error model in locating certain features from their 2-D representation in the pixel array. We concentrate on modeling the error incurred in extracting edges, as edge extraction is a very popular mechanism that is used for both identifying features and also for computing 2-D contours of the objects under observation.

Edge extraction strategies and methods to evaluate their performance qualitatively and quantitatively have been presented and discussed in the literature [1,6,7,9,11,12,13]. There are many types of edges, ideal, ramp and noisy edges are only three of them. Different curvatures in the edges also constitute another dimension to be taken into consideration when it comes to asserting the types of edges that exist.

The goal of developing the error models for edge extraction to to be able assert the following: "Given that the 2-D feature recovered using the edge recovery S is in pixel position (x, y), then there is a probability that the feature was originally at pixel position $(x + 1, y)$ with probability p_1 or .... etc. due to the noise in the pixel image, such that $p_1 + p_2 + ... + p_n = 1$." The problem is to find the probabilities.

It should be obvious that there may be different types of noises and also different levels of those types that might vary at different locations in the sensor image plane. This adds to the different models that we might have to construct. Our approach is to use ideal, that is, synthesized edges of different types, locations and also orientations in image frames then corrupt them with different kinds and levels of noises. As we know the ideal edge points from the ideal image, for which we shall use the edge detector that is to be used in actual experiment to observe a scene. The corrupted images will then be operated upon by the detector and the edge points located. The edge points will differ from the ideal image edge points. The problem reduces to finding corresponding edge points in corrupted and ideal images then finding the error along a large number of edge points. A 2-D histogram is then constructed for the number of points with specific displacement errors from the ideal point. The volume of the histogram is then normalized to be equal to 1, the resulting 3-D function is the 2-D probability density function of the error of displacements. The correspondence between edge points in the corrupted and ideal images is established by choosing the point with the *minimal* distance from the ideal edge point, *such that* it does not correspond to another ideal edge point. The histogram is constructed for each edge and then normalized.

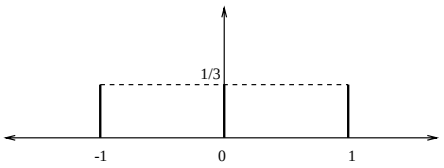

Figure 3: Distribution of the x-Coordinate Displacement

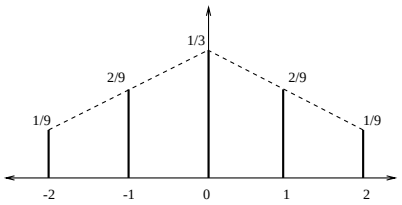

Figure 4: Combined Sensor and Strategy Distribution

2.4 Computing 2-D Motion Uncertainty

In this section we describe how to combine sensor and image processing strategy error models to compute models for the recovered 2-D flow values (difference between locations of features over frames). To simplify the idea, let's assume that we have recovered a specific feature point (x_1, y_1) in an image grabbed at time instant t and the corresponding point (x_2, y_2) at time $t+1$. The problem is to figure out the distribution of v_x. As an example, to explain the procedure, let's assume that from the 3-D sensor distribution we have have computed the marginal density function of the x coordinate of x_1 in the point:

$$f_X(x) = \int_R f_{X,Y}(x,y)dy$$

where R is all the possible y values within the sensor uncertainty model.
The same process is applied for the strategy distribution and another function is recovered. To simplify the process, lets assume that both distributions are identical to the distribution in figure 3, that is, there is an equal probability equal to $\frac{1}{3}$ that the x coordinate is the same, or shifted one position to the left or the right. Combining the spatial information of both distributions as a convolution process would produce the distribution shown in figure 4, which is the error probability density function of having the 3-D feature x 2-D coordinate in the recovered image 2-D x position. Further more, assume that x_2 distribution is the same. The problem reduces to finding the distribution of the optic flow x component, using these two combined distributions. As an example, if $x_1 = 10$ and $x_2 = 22$, then all probability statements can be easily computed, a set of some of these probability statement is shown :

$$P(v_x = 8) = P((x_1 = 12) \wedge (x_2 = 20)) = \frac{1}{9} \times \frac{1}{9} = \frac{1}{81}$$

$$P(v_x = 9) = P(((x_1 = 12) \wedge (x_2 = 21)) \vee ((x_1 = 11) \wedge (x_2 = 20))) = (\frac{1}{9} \times \frac{2}{9}) + (\frac{2}{9} \times \frac{1}{9}) = \frac{4}{81}$$

$$P(v_x = 10 | x_1 = 10) = \frac{P(x_1=10 \wedge x_2=20)}{P(x_1=10)} = \frac{\frac{3}{9} \times \frac{1}{9}}{\frac{3}{9}} = \frac{1}{9}$$

Consequently, all distributions and expected values can be computed from the combination of the sensor level and strategy level uncertainty formulation. In the next section we discuss

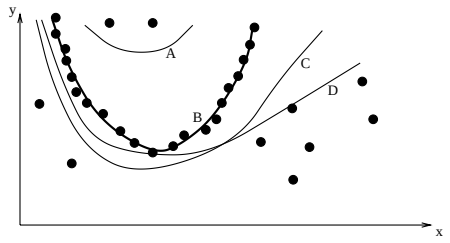

Figure 5: Fitting Parabolic Curves

a method for refining the measured 2-D motion vectors and we then proceed to formulate the 3-D modeling of the scene under observation.

3 Refining Image Motion

In this section we describe a method to refine the recovered 2-D motion vectors on the image plane. Having obtained from the sensor and extraction strategy uncertainty levels distribution estimates for the image flow of the different features, we now try to eliminate the unrealistic ones. We concentrate on the flow estimates for the motion of the scene and develop a technique that is to be used during the observation process as a means to reject faulty estimates. Faulty estimates can results from noise, errors or mistakes in the sensor acquisition process, or visual problems like occlusion, modeling the uncertainties in the previous two levels may still leave room for such anomalies.

Knowing some properties of the scene under observation (mechanical and physical) would help in refining our 2-D estimates. We did a number of experiments to track a robot hand (gripper) performing some manipulation tasks. The features to be tracked on the hand lie on planar surfaces, the modification would be very simple to allow for arbitrary 3-D positions of the feature distribution. Since we know a-priori some information about the mechanical capabilities and limitations and geometric properties of the hand under observation, also about the rate of visual sampling for the camera, we are able to assert some limits on some of the visual parameters in our system.

To illustrate the idea behind the approach, consider figure 5, assume all the curves are 2-D parabolic functions $y = ax^2 + bx + c$, if the set of data points are as shown in the figure, then a least square error fit will produce the function D. However, if we know some upper and lower limits on the values of the coefficients a, b and c then we might be able to construct an upper and lower function parabolas A and C as an enclosing envelope, outside which we can reject all the data points. In that case, we can do a fit for the points that lie inside the envelope and obtain a more realistic function as shown by the curve B.

The situation for rejecting estimates for the image flow of features is not much different. We know the equations that govern the behavior of the image flow as a function of the structure and 3-D motion parameters, as follows :

$$v_x = (1 - px - qy)\left(x\frac{V_Z}{Z_o} - \frac{V_X}{Z_o}\right) +$$

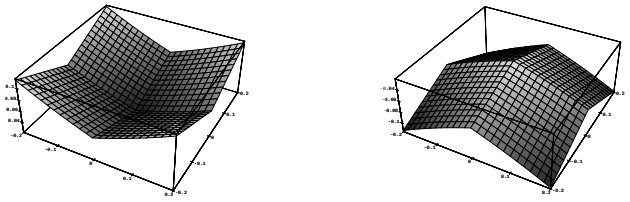

Figure 6: Maximal and Minimal v_x

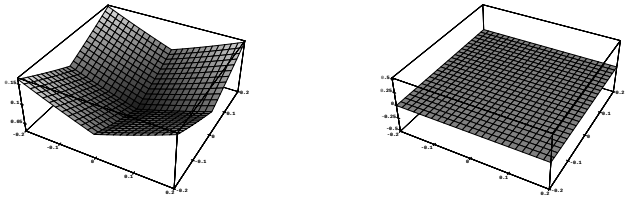

Figure 7: Maximal and Minimal Flow Magnitude

$$\left[xy\Omega_X - \left(1+x^2\right)\Omega_Y + y\Omega_Z\right]$$

$$v_y = (1 - px - qy)\left(y\frac{V_Z}{Z_o} - \frac{V_Y}{Z_o}\right) +$$

$$\left[\left(1+y^2\right)\Omega_X - xy\Omega_Y - x\Omega_Z\right]$$

Which are second degree functions in x and y in three dimensions, $v_x = f_1(x,y)$ and $v_y = f_2(x,y)$.

In addition, we know upper and lower limits on the coefficients p, q, V_X, V_Y, V_Z, Ω_X, Ω_Y, Ω_Z and Z_o (Translational and rotational velocities and structure of the scene), as we know that the mechanical abilities of the robot arm holding the hand will make the relative velocity and distance between the camera impossible to exceed specific values within a visual sampling timing period. So the problem reduces to constructing the three dimensional envelopes for v_x and v_y as the worst case estimates for the flow velocity and rejecting any measured values that lie outside that envelope. Figure 6 indicates the maximal and minimal v_x that can ever be registered on the CCD array of the camera, the x and y are in millimeters and the $x-y$ plane represents the CCD image plane, the depth Z is the maximal v_x in millimeters on the CCD array that can ever be registered. It can be noticed that they are symmetric due to the symmetry in the limits of the coefficients.

As an example, we write the equation governing the maximum v_x value in the first quadrant of the $x-y$ plane (x^+, y^+).

$$v_{x_{max}} = \left(-\frac{fV_{X_s}}{Z_{o_s}} - f\Omega_{Y_s}\right) + \left(\frac{V_{Z_l}}{Z_{o_s}} + \frac{max(p_l V_{X_l}, p_s V_{X_s})}{Z_{o_s}}\right)x$$

$$+ \left(\frac{max(q_l V_{X_l}, q_s V_{X_s})}{Z_{o_s}} + \Omega_{Z_l}\right)y$$

$$+\left(\frac{\Omega_{X_l}}{f}-\frac{min(q_l V_{Z_s}, q_s V_{Z_l})}{f Z_{o_s}}\right) xy$$
$$-\left(\frac{min(p_l V_{Z_s}, p_s V_{Z_l})}{f Z_{o_s}}+\frac{\Omega_{Y_s}}{f}\right) x^2$$

where the subscripts s and l denote lower and upper limits, respectively. At first sight the problem of determining the maximum value of v_x seems to be a constrained non linear optimization problem, which is true, however, assuming that the upper and lower limits of the coefficients are equal in magnitude and opposite in directions (except for Z_o, which is used only as $Z_{o_s}^+$) makes the input to the max and min functions in the above equations always equal and thus providing one more degree of freedom in choosing the parameters and making the choice consistent throughout the equation. Thus the problem becomes simply to write eight equations as the above one for each of v_x and v_y, to draw the function in each of the four quadrants for maximum and minimum envelopes. We shall not rewrite the sixteen equations here, but we show the results for v_x in figure 6, figure 7 represents the maximum and minimum magnitude $m(x, y)$ for the the image flow at any given point, where :

$$m(x, y) = \sqrt{v_x^2 + v_y^2}$$

It should be noted that the maximum absolute possible value of the image flow is minimal at the origin of the camera image plane and increases quadratically as the distance increases from the center.
The above envelopes are then used to reject unrealistic 2-D velocity estimates at different pixel coordinates in the image.

4 Recovering 3-D Uncertainties

We now use the classical formulation for 3-D parameter recovery from 2-D displacement vectors, but using 2-D error distributions as estimates for motion and/or feature coordinates in order to compute 3-D uncertainty distributions for the real world motion vectors and structure instead of singular values for the world parameters.
As an example to illustrate the idea, let's assume that we have a linear system of equations as follows :

$$x + 3y = z_1$$

$$2x + y = z_2$$

The solution of this system is very easily obtained as :

$$x = \frac{3}{5} z_2 - \frac{1}{5} z_1$$

$$y = \frac{2}{5} z_1 - \frac{1}{5} z_2$$

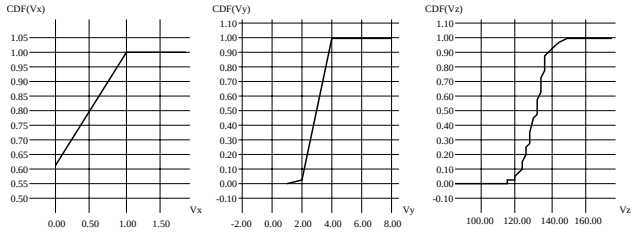

Figure 8: Cumulative Density Functions of the Translational Velocity

That is, a linear combination of the right hand side parameters. If the parameters z_1 and z_2 were random variables of known probability distributions instead of constants, then the problem becomes slightly harder, which is, to find the linear combination of those random variables as another random variable. The obvious way of doing this would be to use convolutions and the formula :

$$P_{X_1+X_2}(y) = \sum_R P_{X_1,X_2}(x, y-x)$$

for the sum of two random variables X_1, X_2 for any real number y and/or the formula for linear combinations over the region R, which is for all x such that $P_{X_1,X_2}(x, y-x) > 0$. Using the moment generating function or the characteristic function seems also to be a very attractive alternative. The moment generating function M of a linear combination of random variables, for example X_1, X_2 can be written as :

$$M_{aX_1+bX_2+c}(t) = e^{ct}\left(M_{X_1}(at)M_{X_2}(bt)\right)$$

for independent random variables X_1, X_2. That is, the problem of solving linear systems on the form $Ax = b$, where b is a vector of random variables, may be reduced to finding closed form solutions for x in terms of the random parameters (using any elimination technique) and then manipulating the results and finding different expectations using moment generating or characteristic functions.

The solutions we suggest to this problem of finding the random variable solution of the 3-D parameters utilize the techniques we described in the previous section. Using either the two-frame iterative technique or the closed form algorithms, it should be noticed that the problem reduces to either solving multi-linear systems or a single one. In that case, using elimination and characteristic functions for computing the required expectations and distributions is straight forward. As an example, the recovered 3-D translational velocity cumulative density functions (CDF) for an actual world motion of the observed gripper in our experiment equal to :

$$V_X = 0\ cm,\ V_Y = 0\ cm \text{ and } V_Z = 13\ cm$$

is shown in figure 8. It should be noted that the recovered distributions represents a fairly accurate estimation of the actual 3-D motion.

Thus, we have suggested algorithms for the estimation of the 3-D uncertainties in the structure and motion of a scene under camera observation.

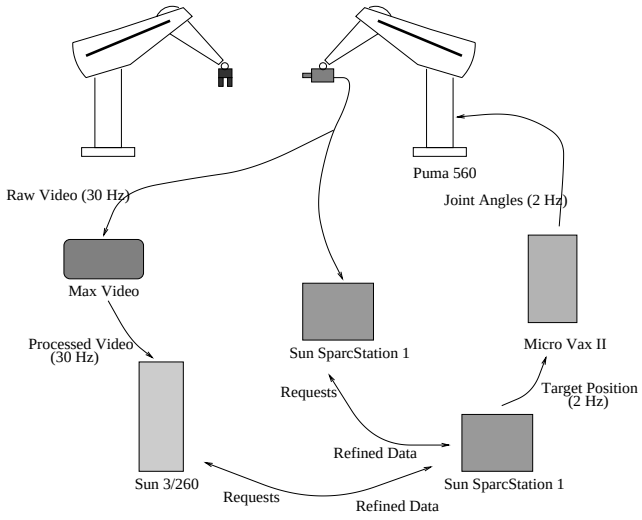

Figure 9: The Architecture of the System

5 The Experimental System

The design and the experiments for the proposed uncertainty recovering formulation were performed on the architecture shown in Figure 9. The agent under observation is the Lord experimental gripper and is mounted on a PUMA 560. The robot and the hand are essentially moved by an external operator to perform some actions on a set of objects lying on a table. The observer sensor is another PUMA 560 on which a camera is mounted. The low level visual feature acquisition is performed on the MaxVideo pipelined video processor at frame rate. In particular, there are two separate paths from the vision sensor. One path is for the computation of the hand 3-D position and orientation and this is done through the MaxVideo. The other path (the inner loop) is done on a SparcStation, in which the image processing modules resides, those modules compute 2-D cues from the scene under observation. Identification of objects, their location with respect to the hand and establishing contact, and correlation procedures are all performed within the inner loop. The 2-D to 3-D conversion and probability computations are performed on another SparcStation. Thus future modifications and enhancements could be coded and executed in a simple and modular fashion. Enhanced Low-level modules for segmentation and 2-D understanding of the image and to accommodate different kinds of objects in the scene could be coded within the inner-loop computer module.

A number of experiments were performed with the lord gripper doing different manipulating action an a set of different objects. Tracking is performed for some features on the gripper, using the MaxVideo system. The visual tracking system works in real time. The 2-D uncertainty levels were tested. Feature extraction with uncertainty is performed using different noise levels, the enclosing "envelopes" were determined for the mechanical system, the rejection algorithms are completed and utilized. The refined and recovered 3-D CDF distribution of uncertainties were then recovered.

Some snap shots depicting the observer view, within an experiment that involves grasping

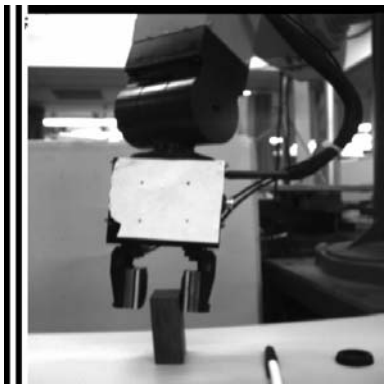

Hand and Objects in Scene
Probability = 0.957878

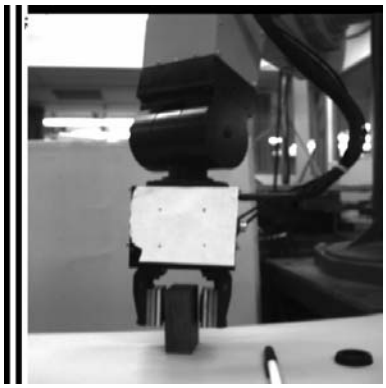

Hand enclosing an Object
Probability = 0.962517

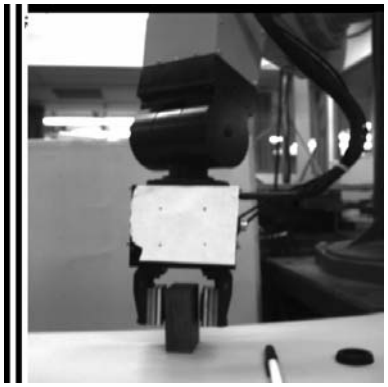

Hand enclosing an Object
Probability = 0.926735

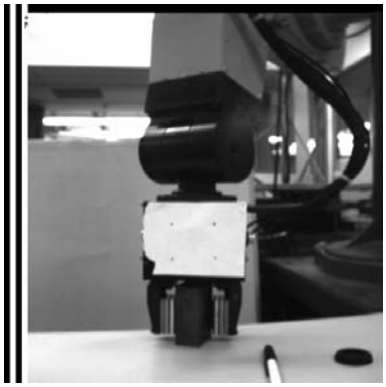

Hand enclosing an Object
Probability = 0.994327

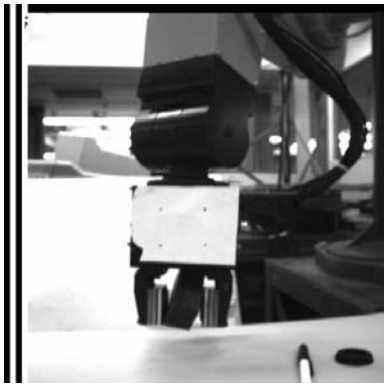

Hand is lifting an Object
Probability = 0.918423

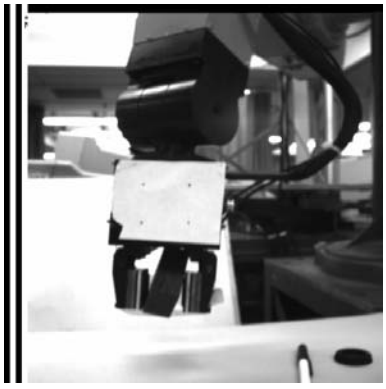

Hand is lifting an Object
Probability = 0.972103

Figure 10: A Manipulation Sequence (Observer View)

and lifting is shown in figure 10. The the corresponding uncertainty in assigning motion and structure values, based on the CDF distribution of the recovered parameters is recovered and displayed.

6 Conclusions

We have described methods to recover the parameters of a scene under observation from sense data *with uncertainty*. We believe that the approach provides for a sensing strategy that *utilizes* knowledge about the sensor errors, the sensory processing uncertainty, and the physical features of the scene under observation. The presented techniques allow the *robust* recovery of the observed environment.

References

[1] I. E. Abdou and W. K. Pratt, "Quantitative Design and Evaluation of Enhancement/Thresholding Edge Detectors", *Proceedings of the IEEE*, Vol. 67, No. 5, May 1979.

[2] H. L. Anderson, *GRASP lab. Camera Systems and Their Effects on Algorithms*, Technical Report MS-CIS-88-85 and GRASP lab. TR 161, University of Pennsylvania, 1988.

[3] R. Bajcsy, E. Krotkov and M. Mintz, *Models of Errors and Mistakes in Machine Perception*, Technical Report MS-CIS-86-26 and GRASP lab. TR 64, University of Pennsylvania, 1986.

[4] N. M. Benahmed, *Camera Calibration for Dynamic Environment*. M.S. Thesis, Department of Electrical Engineering, University of Pennsylvania, 1989.

[5] A. Cameron and H. Wu, "A Framework for Sensory Planning", In *Proceedings of the International Conference on Automation, Robotics and Computer Vision (ICARCV '90)*, Singapore, September 1990.

[6] E. S. Deutsch and J. R. Fram, "A Quantitative Study of the Orientation Bias of some Edge Detector Schemes", *IEEE Trans. Comput.*, C-27, No. 3, March 1978.

[7] J. R. Fram and E. S. Deutsch, "On the Quantitative Evaluation of Edge Detection Schemes and Their Comparison with Human Performance", *IEEE Trans. Comput.*, C-24, No. 6, June 1975.

[8] G. D. Hager, *Active Reduction of Uncertainty in Multi-Sensor Systems*, Ph.D. Thesis, Computer and Information Science Department, University of Pennsylvania, July 1988.

[9] R. M. Haralick and J. S. J. Lee, "Context Dependent Edge Detection and Evaluation", *Pattern Recognition*, Vol. 23, No. 1/2, pp. 1 - 19, 1990.

[10] A. Izaguirre, P. Pu and J. Summers, "A New Development in Camera Calibration: Calibrating a Pair of Mobile Cameras", In *Proceedings of the International Conference on Robotics and Automation*, pp. 74-79, 1985.

[11] L. Kitchen and A. Rosenfeld, "Edge Evaluation Using Local Edge Coherence", *IEEE Transactions on Systems, Man, and Cybernetics*, SMC-11, No. 9, September 1981.

[12] E. Krotkov, *Results in Finding Edges and Corners in Images Using the First Directional Derivative*, Technical Report MS-CIS-85-14 and GRASP lab. TR 37, University of Pennsylvania, 1985.

[13] T. Peli and D. Malah, "A Study of Edge Detection Algorithms", *Computer Graphics and Image Processing*, vol. 20, 1982, pp. 1-21.

[14] R. Y. Tsai, "An Efficient and Accurate Camera Calibration Technique for 3-D Machine Vision", IBM Report.

[15] R. Wilson and G. H. Granlund, "The Uncertainty Principle in Image Processing", IEEE Trans. PAMI, Vol. 6, No. 6, November 1984.

[16] H. Wu and A. Cameron, *A Bayesian Decision Theoretic Approach for Adaptive Goal-directed Sensing*, Technical Report, Philips Laboratories, New York, May 1990.